Supplementary material

Facile Synthesizing Yolk–shelled Fe_3O_4@carbon Nanocavities with Balanced Physiochemical Synergism as Efficient Hosts for High-performance Lithium–sulfur Batteries

Figure S1. The optical photograph of Fe-BTC gel.

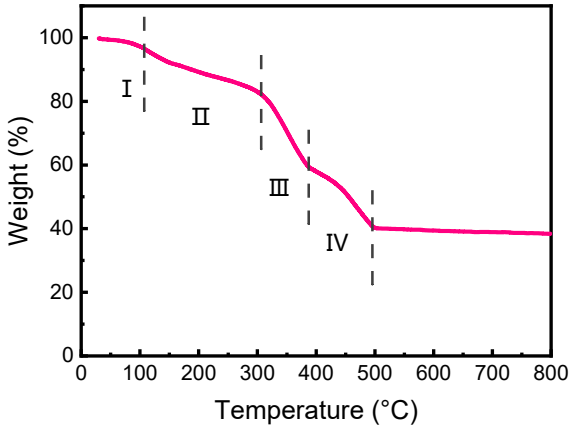

Figure S2. TGA curve of Fe-BTC aerogel acquired in a nitrogen atmosphere.

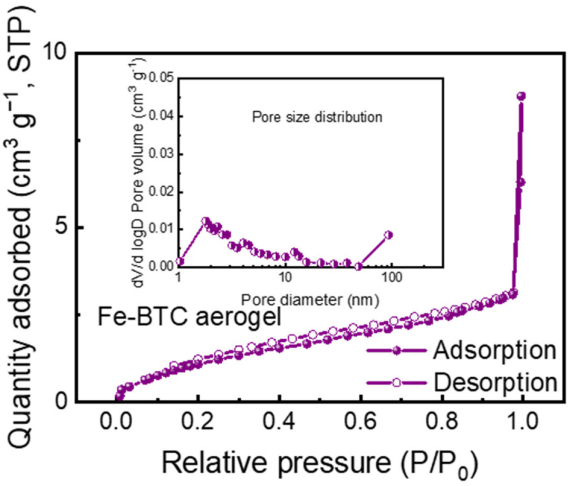

Figure S3. Nitrogen adsorption/desorption isotherm of Fe-BTC aerogel with an inset showing the corresponding size distribution of pores.

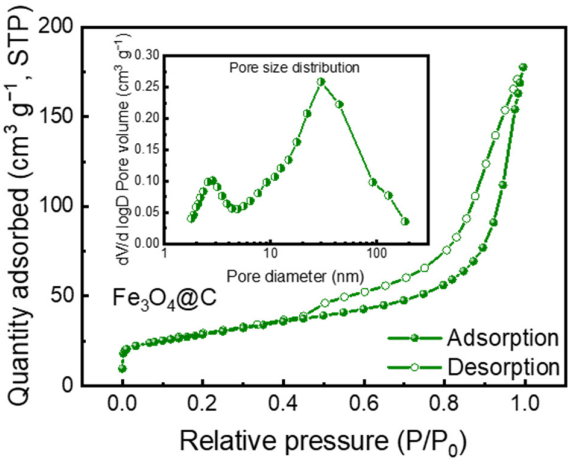

Figure S4. Nitrogen adsorption/desorption isotherm of Fe_3O_4@C with an inset showing the corresponding size distribution of pores.

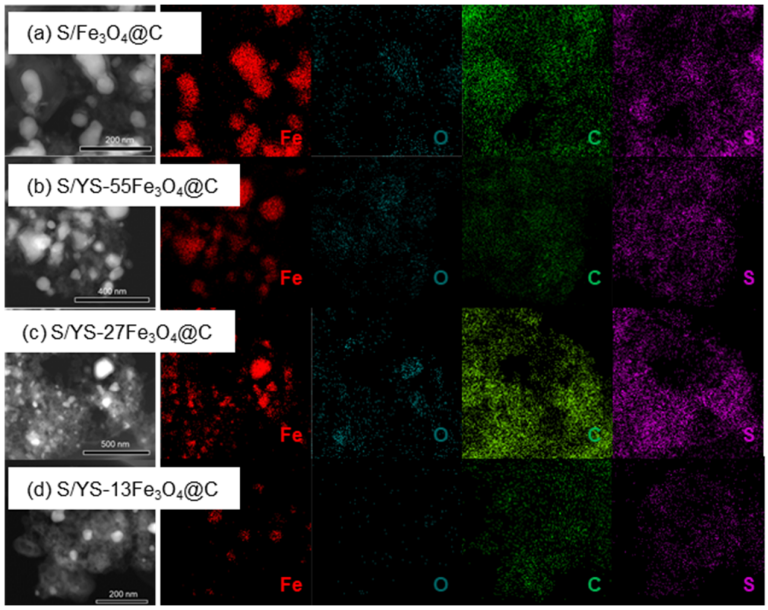

Figure S5. EDS elemental mapping images of (**a**) S/Fe_3O_4@C, (**b**) S/YS-55Fe_3O_4@C, (**c**) S/YS-27Fe_3O_4@C, and (**d**) S/YS-13Fe_3O_4@C.

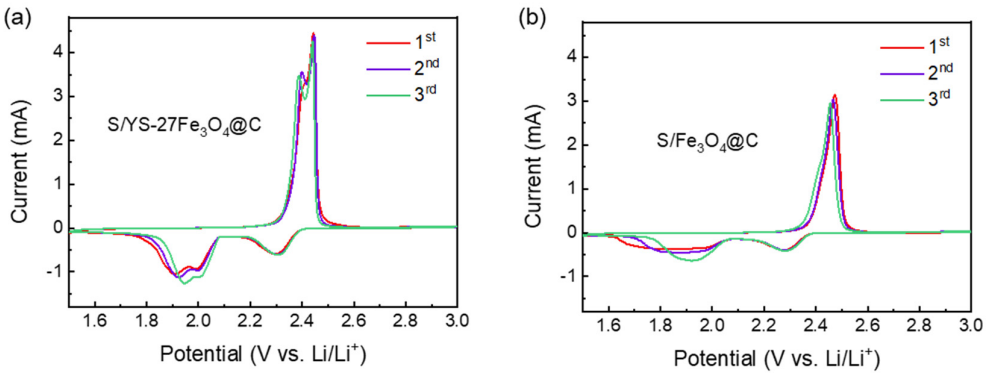

Figure S6. CV curves of (**a**) S/YS-27Fe_3O_4@C and (**b**) S/Fe_3O_4@C at 0.1 mV s^{-1} for different cycles.

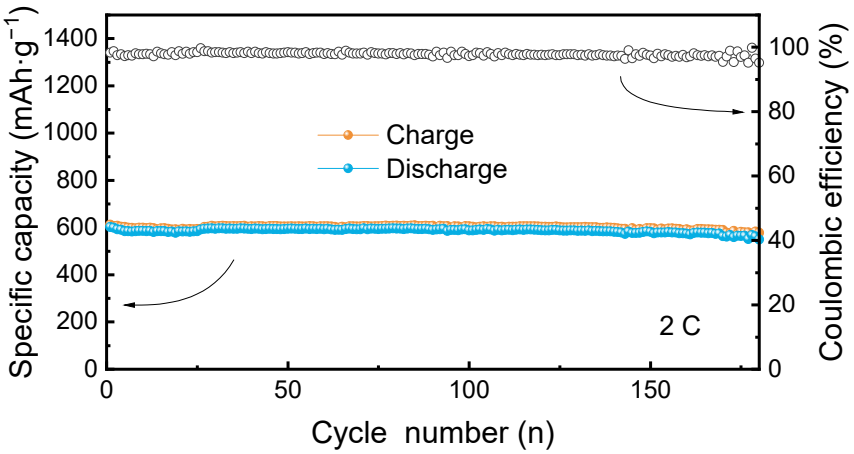

Figure S7. Long-term cycling stability of S/YS-27Fe_3O_4@C electrode at 2 C.

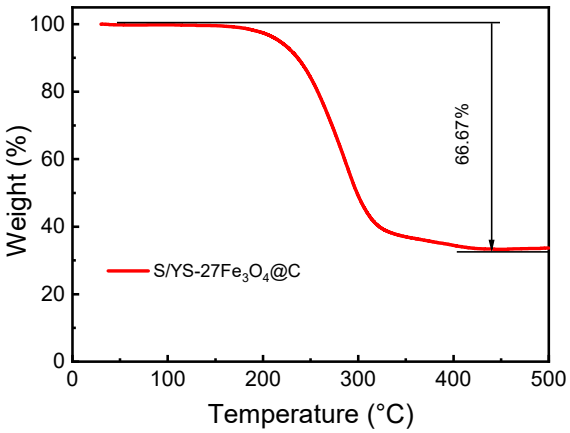

Figure S8. TGA curves of S/YS-27Fe_3O_4@C in N_2.

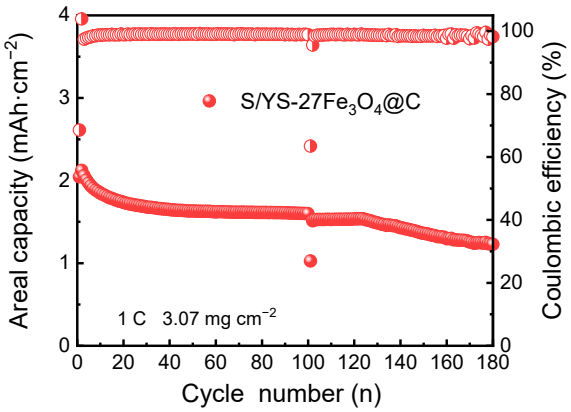

Figure S9. Cycle performance at 1 C of S/YS-27Fe_3O_4@C under high sulfur loadings.

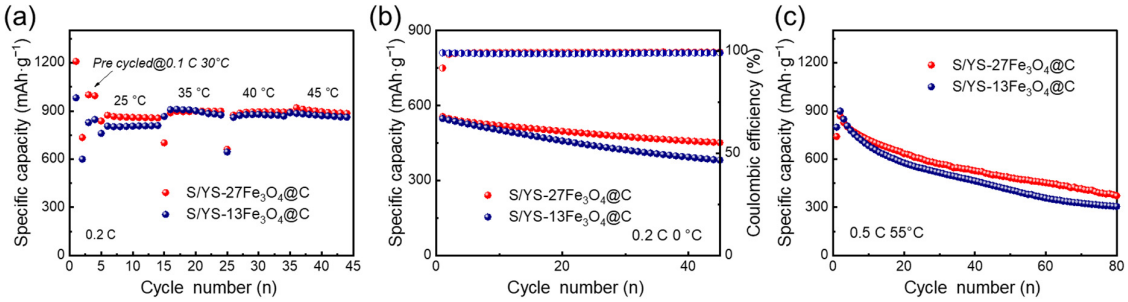

Figure S10. Cycle performance of S/YS-27Fe_3O_4@C and S/YS-13Fe_3O_4@C cathode with a wide temperature range: (a) 25 – 45 °C, (b) 0°C, (c) 55 °C.

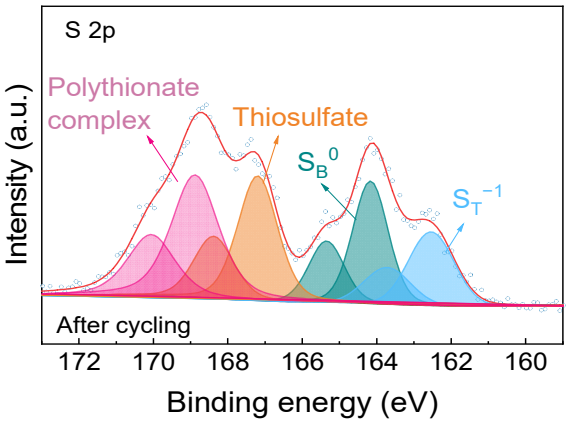

Figure S11. S 2p in S/YS-27Fe_3O_4@C after cycling.

Table S1. Pore structure parameters of Fe-BTC aerogel and Fe_3O_4@C.

	Specific surface area ($m^2\ g^{-1}$)	**Average pore diameter (nm)**	**Pore volume ($cm^3\ g^{-1}$)**
Fe-BTC aerogel	36.1859	2.16362	0.019573
Fe_3O_4@C	99.3583	7.37165	0.183109